

Observation of $D \rightarrow a_0(980)\pi$ in the decays $D^0 \rightarrow \pi^+\pi^-\eta$ and $D^+ \rightarrow \pi^+\pi^0\eta$

 M. Ablikim *et al.**
 (BESIII Collaboration)

 (Received 16 April 2024; accepted 3 December 2024; published 26 December 2024)

We report the first amplitude analyses of the decays $D^0 \rightarrow \pi^+\pi^-\eta$ and $D^+ \rightarrow \pi^+\pi^0\eta$ using a data sample taken with the BESIII detector at the center-of-mass energy of 3773 MeV, corresponding to an integrated luminosity of 7.9 fb^{-1} . The contribution from the process $D^{0(+)} \rightarrow a_0(980)^+\pi^{-(0)}$ is significantly larger than the $D^{0(+)} \rightarrow a_0(980)^{-(0)}\pi^+$ contribution. The ratios $\mathcal{B}(D^0 \rightarrow a_0(980)^+\pi^-)/\mathcal{B}(D^0 \rightarrow a_0(980)^-\pi^+)$ and $\mathcal{B}(D^+ \rightarrow a_0(980)^+\pi^0)/\mathcal{B}(D^+ \rightarrow a_0(980)^0\pi^+)$ are measured to be $7.5_{-0.8\text{stat}}^{+2.5} \pm 1.7_{\text{syst}}$ and $2.6 \pm 0.6_{\text{stat}} \pm 0.3_{\text{syst}}$, respectively. The measured D^0 ratio disagrees with the theoretical predictions by orders of magnitudes, thus implying a substantial contribution from final-state interactions.

 DOI: [10.1103/PhysRevD.110.L111102](https://doi.org/10.1103/PhysRevD.110.L111102)

Theoretical predictions of the strong interaction in the charm sector are challenging, since quantum-chromodynamics calculations involve nonperturbative contributions. In heavy-meson decays, the contributions from W -exchange (WE) and W -annihilation (WA) diagrams are generally expected to be much smaller than that from the color-allowed external W -emission tree (T) diagram. However, in charm-meson decays, these contributions can be significantly enhanced by final-state interactions (FSI). The FSI is nonperturbative and means that there are significant uncertainties when making theoretical predictions of these contributions, since they depend strongly on the cutoff values and the unknown phases between different processes [1,2]. Therefore, the study of decays with a significant contribution from WA or WE processes constitutes a promising method for investigating the dynamics of charm decays.

In the $D \rightarrow SP$ sector (where S and P denote scalar and pseudoscalar particles, respectively), the first indication of the large enhancement of WA diagrams came from the observation of the decays $D_s^+ \rightarrow a_0(980)^{+0}\pi^{0/+}$ and the measurement of the amplitude symmetry $A(D_s^+ \rightarrow a_0(980)^+\pi^0) = -A(D_s^+ \rightarrow a_0(980)^0\pi^+)$ [3]. It has also been noted in Refs. [4,5] that further evidence for the enhancement of WA diagrams through rescattering arises from the observation that the branching fractions (BFs) of $D_s^+ \rightarrow \rho^+\eta^{(\prime)}$ and $D_s^+ \rightarrow \bar{K}^*(892)^0 K^+(K^*(892)^+\bar{K}^0)$ are larger than that of $D_s^+ \rightarrow a^0\pi$. This behavior gives weight

to the interpretation of $a_0(980)$ as a tetraquark or a molecular state [5]. More recently, further measurements involving D_s^+ decays have been performed, in particular those that have led to the observation of the $a_0(1817)^{+(0)}$ resonance [6,7], which is expected to be an excited state of the $a_0(980)^{+(0)}$ [8], supporting the interpretation of these two resonances as $K^{(*)}\bar{K}^{(*)}$ molecules [9,10]. In D^0 decays, both $D^0 \rightarrow a_0(980)^+\pi^-$ and $D^0 \rightarrow a_0(980)^-\pi^+$ only include T and WE processes, which are shown in Fig. 1. The relative ratio $r_{+/-} = \mathcal{B}(D^0 \rightarrow a_0(980)^+\pi^-)/\mathcal{B}(D^0 \rightarrow a_0(980)^-\pi^+)$ is expected to be less than 0.05 [11], when ignoring the WE contribution. Until now, attempts to measure this ratio have been inconclusive: the CLEO and LHCb Collaborations have measured the $a_0(980)^\pm\pi^\mp$ contributions to the decays $D^0 \rightarrow K_S^0 K^\pm\pi^\mp$ [12,13], but with large uncertainties; the Belle Collaboration has studied $D^0 \rightarrow \pi^+\pi^-\eta$ decays [14] but has only observed the $a_0(980)$ peak in the $M(\pi^+\eta)$ projection.

In analogy to what is observed in $D_s^+ \rightarrow a_0(980)^{+(0)}\pi^{0(+)}$ decays [3], substantial contributions from FSI are expected to enhance the WA process in the corresponding D^+ decays. However, in this case the symmetry that is observed in the D_s^+ decays is expected to be violated, since further

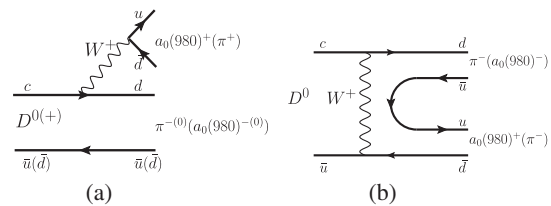


FIG. 1. The diagrams for (a) T and (b) WE diagrams are shown. Here the possible four-quark component for $a_0(980)$ and the gluons are not included.

*Full author list given at the end of the Letter.

short-distance contributions need to be taken into account. The measurement of the BFs for D^0 (D^+) decays to $a_0(980)\pi$ and of the corresponding relative ratios $r_{+/-}$ [$r_{+/-} = \mathcal{B}(D^+ \rightarrow a_0(980)^+\pi^0)/\mathcal{B}(D^+ \rightarrow a_0(980)^0\pi^+)$] can constrain the size and phase of the amplitude of the WE (WA) process and improve the knowledge about the role the $a_0(980)$ plays in charm decays [15].

In this paper, we perform amplitude analyses of $D^{0(+)} \rightarrow \pi^+\pi^{-(0)}\eta$ decays to study the contributions from the intermediate processes $D^{0(+)} \rightarrow a_0(980)^+\pi^{-(0)}$, $D^{0(+)} \rightarrow a_0(980)^{-(0)}\pi^+$, and $D^{0(+)} \rightarrow \rho^{0(+)}\eta$. The analyses are based on e^+e^- collision data recorded with the BESIII detector at a center-of-mass energy of 3773 MeV by employing the process of $e^+e^- \rightarrow \psi(3770) \rightarrow D\bar{D}$, corresponding to an integrated luminosity of 7.9 fb^{-1} [16]. Charge conjugation is implied unless explicitly stated, as are the assumptions that $a_0(980)^{\pm(0)}$ decays to $\pi^{\pm(0)}\eta$ and $\mathcal{B}(a_0(980)^\pm \rightarrow \pi^\pm\eta) = \mathcal{B}(a_0(980)^0 \rightarrow \pi^0\eta)$.

A detailed description of the BESIII detector design and performance can be found in Refs. [17,18]. Simulated data samples are produced with a GEANT4-based [19] package, which includes the geometric description of the BESIII detector and the detector response. These samples are used to determine detection efficiencies and to estimate backgrounds. The simulation models the beam-energy spread and initial-state radiation in e^+e^- annihilations with the generator KKMC [20].

The charged-track selection, particle identification (PID), K_S^0 , π^0 and η reconstruction use the same criteria described in Ref. [3], except for the invariant-mass window around the η , which is set to $450 < M(\gamma\gamma)_\eta < 550 \text{ MeV}/c^2$. The D mesons are identified using the beam-constrained mass $M_{\text{BC}} = \sqrt{E_{\text{beam}}^2 - |\vec{P}_D|^2}$ and the deviation of the reconstructed energy from the expected energy $\Delta E = E_D - E_{\text{beam}}$, where (E_D, \vec{P}_D) is the four-momentum of the D meson and E_{beam} is the beam energy. A double-tag (DT) technique [21] is employed to suppress the background. For the D^0 (D^+) channel, four (six) Cabibbo-allowed decays are used as the tag modes. The collection of events containing tagged $D^{0(+)}$ mesons is referred to as the single-tag (ST) sample [22]. The DT sample is a subset of the ST sample containing events in which the other charm meson is reconstructed decaying into the signal modes. On both sides of the event, any candidate with $M_{\text{BC}} < 1830 \text{ MeV}/c^2$ or $|\Delta E| > 100 \text{ MeV}$ is rejected; if multiple combinations survive, the one with the M_{BC} closest to the known D meson mass from the Particle Data Group (PDG) [23] is retained. Signal simulation samples with $\psi(3770) \rightarrow D\bar{D}$, $\bar{D} \rightarrow \text{tag}$ modes, and $D \rightarrow \text{signal}$ modes are produced, in which the signal decays $D^{0(+)} \rightarrow \pi^+\pi^{-(0)}\eta$ are generated with the amplitude models that result from the studies presented in this paper. On the tag side, the M_{BC} signal windows are set to be

$\pm 6 \text{ MeV}/c^2$ around the known D mass [23], while the ΔE signal windows are set to be 3.5 times the ΔE resolution around the fitted peak. On the signal side, we select D^0 (D^+) candidates with M_{BC} within [1858, 1874] MeV/c^2 ([1860, 1880] MeV/c^2). Furthermore, for the D^0 channel, the requirement $|M(\pi^+\pi^-) - m(K_S^0)| > 30 \text{ MeV}/c^2$ is imposed to remove the peaking background from $D^0 \rightarrow K_S^0\eta$ decays, where $m(K_S^0)$ is the known K_S^0 mass [23]. Since the dominant background originates from wrongly reconstructed $\eta \rightarrow \gamma\gamma$ candidates, a multivariate analysis (MVA) [24] is performed to select events for use in the amplitude analysis. This MVA involves the development of a gradient boosted decision tree (BDTG) classifier based on the inclusive simulation sample, which takes as input three discriminating variables: the $\gamma\gamma$ invariant mass $M(\gamma\gamma)_\eta$, the goodness of the kinematic fit constraining the $\gamma\gamma$ invariant mass to the known η mass $\chi^2(\eta)$, and the helicity angle of the higher-energy photon from the η decay. A requirement on the BDTG output is imposed, which retains 83% (77%) of the signal and rejects 78% (84%) of the background for the D^0 (D^+) channel according to studies performed with simulation samples. Additionally, the selection $|\Delta E| < 45 \text{ MeV}$ ($|\Delta E| < 40 \text{ MeV}$) for the D^0 (D^+) channel is applied. The final sample contains 1678 (1226) $D^0(D^+) \rightarrow \pi^+\pi^-(\pi^0)\eta$ candidates with a purity of $(74.1 \pm 1.2)\%$ [$(65.7 \pm 1.7)\%$]. In these samples 0.4% (0.3%) candidates have been eliminated for the D^0 (D^+) channel due to the best-candidate selection.

The amplitude analysis is performed on the accepted candidate events with an unbinned maximum-likelihood fit. Details on the likelihood construction are given in Sec. I of Supplemental Material [25]. In the likelihood function, the line shape of the $a_0(980)$ is described with Flatté formula. The effective radii for the intermediate resonances and for the $D^{0(+)}$ state are set to be 3.0 and 5.0 GeV^{-1} [26], respectively. The decays $D^0 \rightarrow \rho^0\eta$ and $D^+ \rightarrow a_0(980)^+\pi^0$ are chosen as the reference amplitudes for the D^0 and D^+ channels, with magnitudes and phases set to be 1.0 and 0.0, respectively.

The development of the amplitude models begins by only considering the significant resonances: $a_0(980)^+$ and ρ^0 [$a_0(980)^0$] for D^0 (D^+) channel. Then, various amplitudes are introduced. Only those with significance larger than 3σ are retained for further analysis. Here, the significance is calculated using the changes of $\ln L$ and the number of degrees of freedom (NDF) when the fit is performed with and without the corresponding amplitude included. Following this procedure, six intermediate states are retained in the fit model for both channels. The decay amplitudes and the corresponding phase (ϕ_a), fit fraction (FF_a), significance, BF, and $r_{+/- (0)}$ values are listed in Table I. More details on the interference between the contributions and the correlations are listed in Secs. II and III of Supplemental Material [25], respectively.

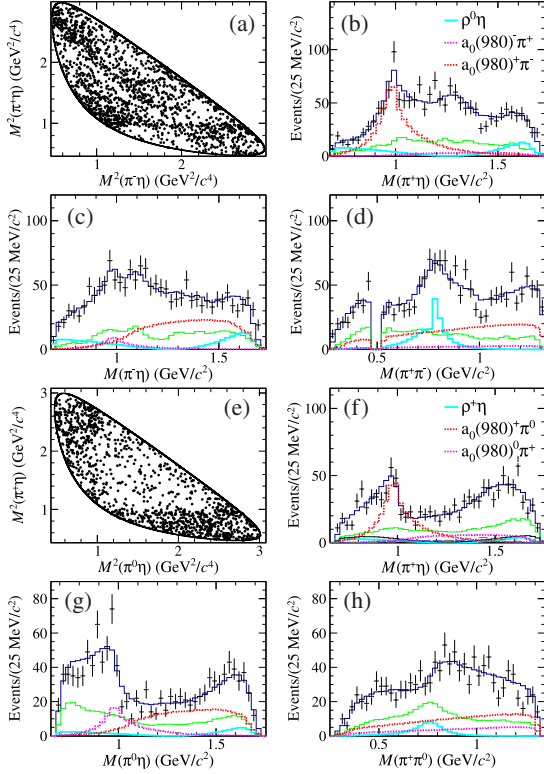


FIG. 2. The Dalitz plot (a); the projections on $M(\pi^+\eta)$ (b), $M(\pi^-\eta)$ (c), and $M(\pi^+\pi^-)$ (d) are for the $D^0 \rightarrow \pi^+\pi^-\eta$ channel. The Dalitz plot (e); the projections on $M(\pi^+\eta)$ (f), $M(\pi^0\eta)$ (g), and $M(\pi^+\pi^0)$ (h) are for the $D^+ \rightarrow \pi^+\pi^0\eta$ channel. In the projections, the dots with error bars are data, the blue lines are the fit curves, and the green histograms are the backgrounds; and the cyan solid, pink dashed and red dashed lines are the contributions from the intermediate states $\rho^{0(+)}$, $a_0(980)^{-(0)}$, and $a_0(980)^+$, respectively. In (d), the events around K_S^0 mass are removed due to the K_S^0 veto.

The Dalitz plots and the projections are shown in Fig. 2. The fit quality is determined by calculating the χ^2 of the fit using an adaptive binning of the Dalitz plots, with each bin containing at least ten events. The resulting χ^2/NDF is 136.6/138 (131.6/99) for the $D^0(D^+)$ channel.

In Table I, the second uncertainties are systematic and arise from the following sources: (I) the coupling with the $\pi\eta'$ channel in the $a_0(980)$ line shape [27]; the parameters for the line shapes of (II) $a_0(980)^\pm$; (III) ρ^0 , $a_2(1320)^+$ and $a_2(1700)^+$ states; and (IV) $(\pi^+\pi^-)_{S\text{-wave}}$ formalism [28]; (V) the effective radii, estimated by varying the effective radii by $\pm 1 \text{ GeV}^{-1}$; (VI) the background level; (VII) the background shape; and (VIII) the fitter performance, estimated by fitting data-sized simulation samples generated with the amplitude models that result from the studies. The fits considered for item (VIII) show good agreement between the fitted and the input values for the parameters in the amplitude model. In addition, the effect from the efficiency variation across the phase space, the efficiency due to PID, tracking, and $\pi^0(\eta)$ reconstruction is found to be negligible. These systematic uncertainties are estimated separately by taking the difference between the values of ϕ_α , FF_α , $r_{+/-}$, and $r_{+/0}$ obtained by the alternative and the baseline fits. Since varying the propagators leads to different normalization factors, only the effect on the FF_α is considered from sources (I) and (IV) for the amplitudes related to the $a_0(980)$ and $(\pi^+\pi^-)_{S\text{-wave}}$. The total systematic uncertainties are obtained by adding each term in quadrature. For $r_{+/-}$, $r_{+/0}$ and the fit fractions of $D \rightarrow a_0(980)\pi$, the sources (I) and (II) are dominant. The detailed results can be found in Tables V and VI in Sec. IV of Supplemental Material [25].

TABLE I. The phases, FFs, statistical significances and BFs for various amplitudes. The first and second uncertainties are statistical and systematic, respectively. The intermediate states are reconstructed in the decays $\rho \rightarrow \pi\pi$, $a_0 \rightarrow \pi\eta$, and $a_2 \rightarrow \pi\eta$.

Amplitude	Phase (in unit rad)	FF (%)	Significance (σ)	BF ($\times 10^{-3}$)
$D^0 \rightarrow \rho^0\eta$	0 (fixed)	$15.2 \pm 1.7 \pm 1.0$	> 10	$0.19 \pm 0.02 \pm 0.01$
$D^0 \rightarrow a_0(980)^-\pi^+$	$0.06 \pm 0.16 \pm 0.12$	$5.9 \pm 1.3 \pm 1.0$	8.9	$0.07 \pm 0.02 \pm 0.01$
$D^0 \rightarrow a_0(980)^+\pi^-$	$-1.06 \pm 0.12 \pm 0.10$	$44.0 \pm 4.0 \pm 5.3$	> 10	$0.55 \pm 0.05 \pm 0.07$
$D^0 \rightarrow a_2(1320)^+\pi^-$	$-1.16 \pm 0.25 \pm 0.23$	$2.1 \pm 0.9 \pm 0.8$	4.5	$0.03 \pm 0.01 \pm 0.01$
$D^0 \rightarrow a_2(1700)^+\pi^-$	$0.08 \pm 0.17 \pm 0.23$	$5.5 \pm 1.8 \pm 2.7$	6.1	$0.07 \pm 0.02 \pm 0.03$
$D^0 \rightarrow (\pi^+\pi^-)_{S\text{-wave}}\eta$	$-0.92 \pm 0.29 \pm 0.14$	$3.9 \pm 1.8 \pm 2.1$	5.3	$0.05 \pm 0.02 \pm 0.03$
$r_{+/-}$		$7.5^{+2.5}_{-0.8} \pm 1.7$	7.7^a	...
$D^+ \rightarrow \rho^+\eta$	$-4.03 \pm 0.19 \pm 0.13$	$9.3 \pm 3.0 \pm 2.1$	6.0	$0.20 \pm 0.07 \pm 0.05$
$D^+ \rightarrow (\pi^+\pi^0)_{\nu}\eta$	$-0.64 \pm 0.22 \pm 0.19$	$15.8 \pm 4.8 \pm 5.2$	4.7	$0.34 \pm 0.11 \pm 0.11$
$D^+ \rightarrow a_0(980)^+\pi^0$	0 (fixed)	$43.7 \pm 5.6 \pm 1.9$	9.1	$0.95 \pm 0.12 \pm 0.05$
$D^+ \rightarrow a_0(980)^0\pi^+$	$2.44 \pm 0.20 \pm 0.10$	$17.0 \pm 4.4 \pm 1.7$	7.9	$0.37 \pm 0.10 \pm 0.04$
$D^+ \rightarrow a_2(1700)^+\pi^0$	$0.92 \pm 0.20 \pm 0.14$	$4.2 \pm 2.1 \pm 0.7$	3.6	$0.09 \pm 0.05 \pm 0.02$
$D^+ \rightarrow a_0(1450)^+\pi^0$	$0.63 \pm 0.41 \pm 0.30$	$7.0 \pm 2.8 \pm 0.7$	4.7	$0.15 \pm 0.06 \pm 0.02$
$r_{+/0}$		$2.6 \pm 0.6 \pm 0.3$	4.0^a	...

^aThe significance is for the test hypothesis $r = 1.0$.

Table I lists the BFs of each subprocess, calculated using $\mathcal{B}_\alpha = \text{FF}_\alpha \times \mathcal{B}(D^{0(+)} \rightarrow \pi^+ \pi^{-(0)} \eta)$. For the BF measurements, we apply tighter selection windows of $505 < M(\gamma\gamma)_\eta < 570$ MeV/ c^2 and $\chi^2(\eta) < 50$ compared to those used for the MVA selections. Using the DT method, the total decay BFs are measured as $\mathcal{B} = Y_{\text{DT}}/Y_{\text{ST}}\epsilon_{\text{sig}}\mathcal{B}_{\text{sub}}$. Here, Y_{ST} is the total ST yield, which is $(6897.1 \pm 8.2) \times 10^3$ [$(4176.9 \pm 2.8) \times 10^3$] for the D^0 (D^+) channel; \mathcal{B}_{sub} is the BF of $\pi^0(\eta) \rightarrow \gamma\gamma$; and ϵ_{sig} is the weighted signal efficiency $\epsilon_{\text{sig}} = \sum_i \frac{Y_{\text{ST}}^{(i)}}{\epsilon_{\text{ST}}^{(i)}} \epsilon_{\text{DT}}^{(i)}/Y_{\text{ST}}$, where $Y_{\text{ST}}^{(i)}$ and $\epsilon_{\text{ST}}^{(i)}$ are the ST yield and ST (DT) efficiencies for the i th tag channels, respectively. The DT yields Y_{DT} are determined using a fit to the ΔE distributions as reported in Sec. V of Supplemental Material [25]. We obtain $Y_{\text{DT}}(D^0) = 1369 \pm 48$ and $Y_{\text{DT}}(D^+) = 949 \pm 54$. The total BFs of the $D^0 \rightarrow \pi^+ \pi^- \eta$ and $D^+ \rightarrow \pi^+ \pi^0 \eta$ channels are measured to be $(1.24 \pm 0.04_{\text{stat}} \pm 0.03_{\text{syst}}) \times 10^{-3}$ and $(2.18 \pm 0.12_{\text{stat}} \pm 0.05_{\text{syst}}) \times 10^{-3}$, respectively. Here, the systematic uncertainties for the D^0 and D^+ channels include contributions associated with: PID (1.0% and 0.5%); tracking efficiency (1.0% and 0.5%); η/π^0 reconstruction (0.8% and 1.6%), determined from hadronic DT $D\bar{D}$ events; the choice of signal shape (0.3% and 0.1%), estimated from the change in Y_{DT} when altering the parameters in the signal shape within the uncertainties; the choice of background shape (0.6% and 1.4%), estimated by using a third-order Chebyshev polynomial instead of the second-order one; the choice of M_{BC} window (0.3% and 0.0%), determined with a $D^0 \rightarrow K^- \pi^+ \eta$ control sample for the D^0 channel and found to be negligible for the D^+ channel due to the looser requirement; the simulation sample size (0.1% and 0.1%); the effect of quantum correlations in the D^0 channel (0.9%) [29]; possible fitter biases (0.3% and 0.6%), estimated from the inclusive simulation sample; the generator (0.2% and 0.4%), estimated by varying the input parameters in the generator according to the error matrix obtained from the fit to data; and uncertainties from $\mathcal{B}(\eta/\pi^0 \rightarrow \gamma\gamma)$ (0.5% and 0.5%), as taken from the PDG [23].

In summary, we have presented the first amplitude analysis of the $D^{0(+)} \rightarrow \pi^+ \pi^{-(0)} \eta$ decay. The decays $D^{0(+)} \rightarrow a_0(980)^+ \pi^{-(0)}$ and $D^{0(+)} \rightarrow a_0(980)^{-(0)} \pi^+$ are observed for the first time, with statistical significances $> 10\sigma$ (9.1σ) and 8.9σ (7.9σ), respectively. The $a_0(980)^+$ is identified as the dominant intermediate resonance in both channels, with its contribution significantly larger than that of the $a_0(980)^{-(0)}$ state. The measured values of $r_{+/-} = 7.5_{-0.8}^{+2.5} \pm 1.7$ and $r_{+/0} = 2.6 \pm 0.6 \pm 0.3$ indicate that the symmetry observed in D_s^+ decays is violated here. Furthermore, the low BF of $D^{0(+)} \rightarrow \rho^{0(+)} \eta$ highlights the importance of the $K^* K \rightarrow a_0(980) \pi$ rescattering process.

The value of $r_{+/-}$ determined from the amplitude model is found to be 2 orders of magnitude higher than the expectation without contributions from WE diagrams [11]. This suggests that under the conventional diquark model for the $a_0(980)$, the WE diagrams are significantly enhanced. A simple calculation outlined in Sec. VI of Supplemental Material [25] predicts the size of the WE diagram to exceed that of the T diagram. Specifically, for $D^0 \rightarrow a_0(980)^+ \pi^-$, the WE diagram is expected to be more than $\sqrt{6.0}$ times larger than that of the T diagram. In contrast to the $D \rightarrow PP$ and $D \rightarrow VP$ decay sectors, where T diagrams dominate over WE diagrams, the weak-annihilation process significantly enhanced by FSI is a unique feature of $D \rightarrow SP$ decays. When only considering the WE diagrams, the estimation in Sec. VI of Supplemental Material [25] predicts $r_{+/-} \sim 0.3$, which contradicts the measurement. This leads to the conclusion that the phase and magnitude of the WE diagrams in $D^0 \rightarrow a_0(980)^- \pi^+$ must produce strong interference effects that enhance the ratio of $r_{+/-}$.

Assuming a four-quark model for $a_0(980)$, the decay $D^0 \rightarrow a_0(980)^+ \pi^-$ receives an additional contribution from a T-like diagram significantly larger than the T diagram shown in Fig. 1(a). In this case, the ratio $r_{+/-}$ can be greatly enhanced without the fine-tuned WE contributions needed in the two-quark model. Thus, the results presented in this paper, combined with future determinations of the magnitude and phase of the WE diagrams in other $D \rightarrow SP$ decays, will be valuable in improving our understanding of the internal structure of the $a_0(980)$ meson.

The authors greatly thank Professor H. Y. Cheng from Institute of Physics, Academia Sinica for the useful discussions. The BESIII Collaboration thanks the staff of BEPCII and the IHEP computing center for their strong support. This work is supported in part by National Key R&D Program of China under Contracts No. 2023YFA1606000, No. 2020YFA0406400, and No. 2020YFA0406300; National Natural Science Foundation of China (NSFC) under Contracts No. 12205384, No. 11635010, No. 11735014, No. 11935015, No. 11935016, No. 11935018, No. 11961141012, No. 12025502, No. 12035009, No. 12035013, No. 12061131003, No. 12192260, No. 12192261, No. 12192262, No. 12192263, No. 12192264, No. 12192265, No. 12221005, No. 12225509, No. 12235017, and No. 12361141819; the Chinese Academy of Sciences (CAS) Large-Scale Scientific Facility Program; the CAS Center for Excellence in Particle Physics (CCEPP); Joint Large-Scale Scientific Facility Funds of the NSFC and CAS under Contracts No. U1832207 and No. U2032104; 100 Talents Program of CAS; The Excellent Youth Foundation of Henan Scientific Committee under Contract No. 242300421044; The Institute of Nuclear and Particle Physics (INPAC) and Shanghai Key Laboratory for Particle Physics and Cosmology; German Research

Foundation DFG under Contracts No. 455635585, No. FOR5327, and No. GRK 2149; Istituto Nazionale di Fisica Nucleare, Italy; Ministry of Development of Turkey under Contract No. DPT2006K-120470; National Research Foundation of Korea under Contract No. NRF-2022R1A2C1092335; National Science and Technology fund of Mongolia; National Science Research and

Innovation Fund (NSRF) via the Program Management Unit for Human Resources & Institutional Development, Research and Innovation of Thailand under Contract No. B16F640076; Polish National Science Centre under Contract No. 2019/35/O/ST2/02907; The Swedish Research Council; and U.S. Department of Energy under Contract No. DE-FG02-05ER41374.

-
- [1] H. Y. Cheng and C. W. Chiang, *Phys. Rev. D* **81**, 074021 (2010).
- [2] Q. Qin, H. n. Li, C. D. Lü, and F. S. Yu, *Phys. Rev. D* **89**, 054006 (2014).
- [3] M. Ablikim *et al.* (BESIII Collaboration), *Phys. Rev. Lett.* **123**, 112001 (2019).
- [4] Y. K. Hsiao, Y. Yu, and B. C. Ke, *Eur. Phys. J. C* **80**, 895 (2020).
- [5] X. Z. Ling, M. Z. Liu, J. X. Lu, L. S. Geng, and J. J. Xie, *Phys. Rev. D* **103**, 116016 (2021).
- [6] M. Ablikim *et al.* (BESIII Collaboration), *Phys. Rev. D* **105**, L051103 (2022).
- [7] M. Ablikim *et al.* (BESIII Collaboration), *Phys. Rev. Lett.* **129**, 182001 (2022).
- [8] D. Guo, W. Chen, H. X. Chen, X. Liu, and S. L. Zhu, *Phys. Rev. D* **105**, 114014 (2022).
- [9] Z. L. Wang and B. S. Zou, *Phys. Rev. D* **104**, 114001 (2021).
- [10] E. Oset, L. R. Dai, and L. S. Geng, *Sci. Bull.* **68**, 243 (2023).
- [11] H. Y. Cheng, C. W. Chiang, and Z. Q. Zhang, *Phys. Rev. D* **105**, 033006 (2022).
- [12] J. Insler (CLEO Collaboration), *Phys. Rev. D* **85**, 092016 (2012); **94**, 099905(E) (2016).
- [13] R. Aaij *et al.* (LHCb Collaboration), *Phys. Rev. D* **93**, 052018 (2016).
- [14] L. K. Li *et al.* (Belle Collaboration), *J. High Energy Phys.* **09** (2021) 075.
- [15] N. Ikeno, M. Bayar, and E. Oset, *Eur. Phys. J. C* **81**, 377 (2021).
- [16] M. Ablikim *et al.* (BESIII Collaboration), *Chin. Phys. C* **48**, 123001 (2024).
- [17] M. Ablikim *et al.* (BESIII Collaboration), *Nucl. Instrum. Methods Phys. Res., Sect. A* **614**, 345 (2010).
- [18] X. Li *et al.*, *Radiat. Detect. Technol. Methods* **1**, 13 (2017); Y. X. Guo *et al.*, *Radiat. Detect. Technol. Methods* **1**, 15 (2017); P. Cao *et al.*, *Nucl. Instrum. Methods Phys. Res., Sect. A* **953**, 163053 (2020); *J. Instrum.* **11**, C08009 (2016).
- [19] S. Agostinelli *et al.* (Geant4 Collaboration), *Nucl. Instrum. Methods Phys. Res., Sect. A* **506**, 250 (2003).
- [20] S. Jadach, B. F. L. Ward, and Z. Was, *Phys. Rev. D* **63**, 113009 (2001); *Comput. Phys. Commun.* **130**, 260 (2000).
- [21] R. M. Baltrusaitis *et al.* (MARK-III Collaboration), *Phys. Rev. Lett.* **56**, 2140 (1986).
- [22] The used tag modes are $D^0 \rightarrow K^- \pi^+$, $D^0 \rightarrow K^- \pi^+ \pi^0$, $D^0 \rightarrow K^- \pi^+ \pi^0 \pi^0$, $D^0 \rightarrow K^- \pi^+ \pi^+ \pi^-$, $D^+ \rightarrow K^- \pi^+ \pi^+$, $D^+ \rightarrow K^- \pi^+ \pi^+ \pi^0$, $D^+ \rightarrow K_S^0 \pi^+$, $D^+ \rightarrow K_S^0 \pi^+ \pi^0$, $D^+ \rightarrow K_S^0 \pi^+ \pi^+ \pi^-$, and $D^+ \rightarrow K^- K^+ \pi^+$.
- [23] R. L. Workman *et al.* (Particle Data Group), *Prog. Theor. Exp. Phys.* **2022**, 083C01 (2022).
- [24] A. Hocker *et al.*, *Proc. Sci. ACAT2007* (2007) 040 [arXiv: physics/0703039].
- [25] See Supplemental Material at <http://link.aps.org/supplemental/10.1103/PhysRevD.110.L111102> for detailed information for the analysis of $D^{0/+} \rightarrow \pi^+ \pi^{-/0} \eta$.
- [26] M. Ablikim *et al.* (BESIII Collaboration), *Phys. Rev. D* **95**, 072010 (2017).
- [27] M. Ablikim *et al.* (BESIII Collaboration), *Phys. Rev. D* **95**, 032002 (2017).
- [28] R. Aaij *et al.* (LHCb Collaboration), *Phys. Rev. D* **92**, 032002 (2015).
- [29] M. Ablikim *et al.* (BESIII Collaboration), *Phys. Rev. D* **101**, 052009 (2020).

M. Ablikim,¹ M. N. Achasov,^{4,c} P. Adlarson,⁷⁵ O. Afedulidis,³ X. C. Ai,⁸⁰ R. Aliberti,³⁵ A. Amoroso,^{74a,74c} Q. An,^{71,58,a} Y. Bai,⁵⁷ O. Bakina,³⁶ I. Balossino,^{29a} Y. Ban,^{46,h} H.-R. Bao,⁶³ V. Batozskaya,^{1,44} K. Begzsuren,³² N. Berger,³⁵ M. Berlowski,⁴⁴ M. Bertani,^{28a} D. Bettoni,^{29a} F. Bianchi,^{74a,74c} E. Bianco,^{74a,74c} A. Bortone,^{74a,74c} I. Boyko,³⁶ R. A. Briere,⁵ A. Brueggemann,⁶⁸ H. Cai,⁷⁶ X. Cai,^{1,58} A. Calcaterra,^{28a} G. F. Cao,^{1,63} N. Cao,^{1,63} S. A. Cetin,^{62a} J. F. Chang,^{1,58} G. R. Che,⁴³ G. Chelkov,^{36,b} C. Chen,⁴³ C. H. Chen,⁹ Chao Chen,⁵⁵ G. Chen,¹ H. S. Chen,^{1,63} H. Y. Chen,²⁰ M. L. Chen,^{1,58,63} S. J. Chen,⁴² S. L. Chen,⁴⁵ S. M. Chen,⁶¹ T. Chen,^{1,63} X. R. Chen,^{31,63} X. T. Chen,^{1,63} Y. B. Chen,^{1,58} Y. Q. Chen,³⁴ Z. J. Chen,^{25,i} Z. Y. Chen,^{1,63} S. K. Choi,¹⁰ G. Cibinetto,^{29a} F. Cossio,^{74c} J. J. Cui,⁵⁰ H. L. Dai,^{1,58} J. P. Dai,⁷⁸ A. Dbeyssi,¹⁸ R. E. de Boer,³ D. Dedovich,³⁶ C. Q. Deng,⁷² Z. Y. Deng,¹ A. Denig,³⁵ I. Denysenko,³⁶ M. Destefanis,^{74a,74c} F. De Mori,^{74a,74c} B. Ding,^{66,1} X. X. Ding,^{46,h} Y. Ding,³⁴ Y. Ding,⁴⁰ J. Dong,^{1,58} L. Y. Dong,^{1,63} M. Y. Dong,^{1,58,63} X. Dong,⁷⁶

M. C. Du,¹ S. X. Du,⁸⁰ Y. Y. Duan,⁵⁵ Z. H. Duan,⁴² P. Egorov,^{36,b} Y. H. Fan,⁴⁵ J. Fang,⁵⁹ J. Fang,^{1,58} S. S. Fang,^{1,63}
 W. X. Fang,¹ Y. Fang,¹ Y. Q. Fang,^{1,58} R. Farinelli,^{29a} L. Fava,^{74b,74c} F. Feldbauer,³ G. Felici,^{28a} C. Q. Feng,^{71,58} J. H. Feng,⁵⁹
 Y. T. Feng,^{71,58} M. Fritsch,³ C. D. Fu,¹ J. L. Fu,⁶³ Y. W. Fu,^{1,63} H. Gao,⁶³ X. B. Gao,⁴¹ Y. N. Gao,^{46,h} Yang Gao,^{71,58}
 S. Garbolino,^{74c} I. Garzia,^{29a,29b} L. Ge,⁸⁰ P. T. Ge,⁷⁶ Z. W. Ge,⁴² C. Geng,⁵⁹ E. M. Gersabeck,⁶⁷ A. Gilman,⁶⁹ K. Goetzen,¹³
 L. Gong,⁴⁰ W. X. Gong,^{1,58} W. Gradl,³⁵ S. Gramigna,^{29a,29b} M. Greco,^{74a,74c} M. H. Gu,^{1,58} Y. T. Gu,¹⁵ C. Y. Guan,^{1,63}
 A. Q. Guo,^{31,63} L. B. Guo,⁴¹ M. J. Guo,⁵⁰ R. P. Guo,⁴⁹ Y. P. Guo,^{12,g} A. Guskov,^{36,b} J. Gutierrez,²⁷ K. L. Han,⁶³ T. T. Han,¹
 F. Hanisch,³ X. Q. Hao,¹⁹ F. A. Harris,⁶⁵ K. K. He,⁵⁵ K. L. He,^{1,63} F. H. Heinsius,³ C. H. Heinz,³⁵ Y. K. Heng,^{1,58,63}
 C. Herold,⁶⁰ T. Holtmann,³ P. C. Hong,³⁴ G. Y. Hou,^{1,63} X. T. Hou,^{1,63} Y. R. Hou,⁶³ Z. L. Hou,¹ B. Y. Hu,⁵⁹ H. M. Hu,^{1,63}
 J. F. Hu,^{56,j} S. L. Hu,^{12,g} T. Hu,^{1,58,63} Y. Hu,¹ G. S. Huang,^{71,58} K. X. Huang,⁵⁹ L. Q. Huang,^{31,63} X. T. Huang,⁵⁰ Y. P. Huang,¹
 Y. S. Huang,⁵⁹ T. Hussain,⁷³ F. Hölzken,³ N. Hüsken,³⁵ N. in der Wiesche,⁶⁸ J. Jackson,²⁷ S. Janchiv,³² J. H. Jeong,¹⁰ Q. Ji,¹
 Q. P. Ji,¹⁹ W. Ji,^{1,63} X. B. Ji,^{1,63} X. L. Ji,^{1,58} Y. Y. Ji,⁵⁰ X. Q. Jia,⁵⁰ Z. K. Jia,^{71,58} D. Jiang,^{1,63} H. B. Jiang,⁷⁶ P. C. Jiang,^{46,h}
 S. S. Jiang,³⁹ T. J. Jiang,¹⁶ X. S. Jiang,^{1,58,63} Y. Jiang,⁶³ J. B. Jiao,⁵⁰ J. K. Jiao,³⁴ Z. Jiao,²³ S. Jin,⁴² Y. Jin,⁶⁶ M. Q. Jing,^{1,63}
 X. M. Jing,⁶³ T. Johansson,⁷⁵ S. Kabana,³³ N. Kalantar-Nayestanaki,⁶⁴ X. L. Kang,⁹ X. S. Kang,⁴⁰ M. Kavatsyuk,⁶⁴
 B. C. Ke,⁸⁰ V. Khachatryan,²⁷ A. Khoukaz,⁶⁸ R. Kiuchi,¹ O. B. Kolcu,^{62a} B. Kopf,³ M. Kuessner,³ X. Kui,^{1,63} N. Kumar,²⁶
 A. Kupsc,^{44,75} W. Kühn,³⁷ J. J. Lane,⁶⁷ L. Lavezzi,^{74a,74c} T. T. Lei,^{71,58} Z. H. Lei,^{71,58} M. Lellmann,³⁵ T. Lenz,³⁵ C. Li,⁴⁷
 C. Li,⁴³ C. H. Li,³⁹ Cheng Li,^{71,58} D. M. Li,⁸⁰ F. Li,^{1,58} G. Li,¹ H. B. Li,^{1,63} H. J. Li,¹⁹ H. N. Li,^{56,j} Hui Li,⁴³ J. R. Li,⁶¹
 J. S. Li,⁵⁹ K. Li,¹ L. J. Li,^{1,63} L. K. Li,¹ Lei Li,⁴⁸ M. H. Li,⁴³ P. R. Li,^{38,k,l} Q. M. Li,^{1,63} Q. X. Li,⁵⁰ R. Li,^{17,31} S. X. Li,¹² T. Li,⁵⁰
 W. D. Li,^{1,63} W. G. Li,^{1,a} X. Li,^{1,63} X. H. Li,^{71,58} X. L. Li,⁵⁰ X. Y. Li,^{1,63} X. Z. Li,⁵⁹ Y. G. Li,^{46,h} Z. J. Li,⁵⁹ Z. Y. Li,⁷⁸
 C. Liang,⁴² H. Liang,^{1,63} H. Liang,^{71,58} Y. F. Liang,⁵⁴ Y. T. Liang,^{31,63} G. R. Liao,¹⁴ Y. P. Liao,^{1,63} J. Libby,²⁶ A. Limphirat,⁶⁰
 C. C. Lin,⁵⁵ D. X. Lin,^{31,63} T. Lin,¹ B. J. Liu,¹ B. X. Liu,⁷⁶ C. Liu,³⁴ C. X. Liu,¹ F. Liu,¹ F. H. Liu,⁵³ Feng Liu,⁶ G. M. Liu,^{56,j}
 H. Liu,^{38,k,l} H. B. Liu,¹⁵ H. H. Liu,¹ H. M. Liu,^{1,63} Huihui Liu,²¹ J. B. Liu,^{71,58} J. Y. Liu,^{1,63} K. Liu,^{38,k,l} K. Y. Liu,⁴⁰ Ke Liu,²²
 L. Liu,^{71,58} L. C. Liu,⁴³ Lu Liu,⁴³ M. H. Liu,^{12,g} P. L. Liu,¹ Q. Liu,⁶³ S. B. Liu,^{71,58} T. Liu,^{12,g} W. K. Liu,⁴³ W. M. Liu,^{71,58}
 X. Liu,^{38,k,l} X. Liu,³⁹ Y. Liu,⁸⁰ Y. Liu,^{38,k,l} Y. B. Liu,⁴³ Z. A. Liu,^{1,58,63} Z. D. Liu,⁹ Z. Q. Liu,⁵⁰ X. C. Lou,^{1,58,63} F. X. Lu,⁵⁹
 H. J. Lu,²³ J. G. Lu,^{1,58} X. L. Lu,¹ Y. Lu,⁷ Y. P. Lu,^{1,58} Z. H. Lu,^{1,63} C. L. Luo,⁴¹ J. R. Luo,⁵⁹ M. X. Luo,⁷⁹ T. Luo,^{12,g}
 X. L. Luo,^{1,58} X. R. Lyu,⁶³ Y. F. Lyu,⁴³ F. C. Ma,⁴⁰ H. Ma,⁷⁸ H. L. Ma,¹ J. L. Ma,^{1,63} L. L. Ma,⁵⁰ M. M. Ma,^{1,63} Q. M. Ma,¹
 R. Q. Ma,^{1,63} T. Ma,^{71,58} X. T. Ma,^{1,63} X. Y. Ma,^{1,58} Y. Ma,^{46,h} Y. M. Ma,³¹ F. E. Maas,¹⁸ M. Maggiora,^{74a,74c} S. Malde,⁶⁹
 Y. J. Mao,^{46,h} Z. P. Mao,¹ S. Marcello,^{74a,74c} Z. X. Meng,⁶⁶ J. G. Messchendorp,^{13,64} G. Mezzadri,^{29a} H. Miao,^{1,63} T. J. Min,⁴²
 R. E. Mitchell,²⁷ X. H. Mo,^{1,58,63} B. Moses,²⁷ N. Yu. Muchnoi,^{4,c} J. Muskalla,³⁵ Y. Nefedov,³⁶ F. Nerling,^{18,e} L. S. Nie,²⁰
 I. B. Nikolaev,^{4,c} Z. Ning,^{1,58} S. Nisar,^{11,m} Q. L. Niu,^{38,k,l} W. D. Niu,⁵⁵ Y. Niu,⁵⁰ S. L. Olsen,⁶³ Q. Ouyang,^{1,58,63}
 S. Pacetti,^{28b,28c} X. Pan,⁵⁵ Y. Pan,⁵⁷ A. Pathak,³⁴ Y. P. Pei,^{71,58} M. Pelizaeus,³ H. P. Peng,^{71,58} Y. Y. Peng,^{38,k,l} K. Peters,^{13,e}
 J. L. Ping,⁴¹ R. G. Ping,^{1,63} S. Plura,³⁵ V. Prasad,³³ F. Z. Qi,¹ H. Qi,^{71,58} H. R. Qi,⁶¹ M. Qi,⁴² T. Y. Qi,^{12,g} S. Qian,^{1,58}
 W. B. Qian,⁶³ C. F. Qiao,⁶³ X. K. Qiao,⁸⁰ J. J. Qin,⁷² L. Q. Qin,¹⁴ L. Y. Qin,^{71,58} X. P. Qin,^{12,g} X. S. Qin,⁵⁰ Z. H. Qin,^{1,58}
 J. F. Qiu,¹ Z. H. Qu,⁷² C. F. Redmer,³⁵ K. J. Ren,³⁹ A. Rivetti,^{74c} M. Rolo,^{74c} G. Rong,^{1,63} Ch. Rosner,¹⁸ S. N. Ruan,⁴³
 N. Salone,⁴⁴ A. Sarantsev,^{36,d} Y. Schelhaas,³⁵ K. Schoenning,⁷⁵ M. Scodreggio,^{29a} K. Y. Shan,^{12,g} W. Shan,²⁴ X. Y. Shan,^{71,58}
 Z. J. Shang,^{38,k,l} J. F. Shangguan,¹⁶ L. G. Shao,^{1,63} M. Shao,^{71,58} C. P. Shen,^{12,g} H. F. Shen,^{1,8} W. H. Shen,⁶³ X. Y. Shen,^{1,63}
 B. A. Shi,⁶³ H. Shi,^{71,58} H. C. Shi,^{71,58} J. L. Shi,^{12,g} J. Y. Shi,¹ Q. Q. Shi,⁵⁵ S. Y. Shi,⁷² X. Shi,^{1,58} J. J. Song,¹⁹ T. Z. Song,⁵⁹
 W. M. Song,^{34,1} Y. J. Song,^{12,g} Y. X. Song,^{46,h,n} S. Sosio,^{74a,74c} S. Spataro,^{74a,74c} F. Stieler,³⁵ Y. J. Su,⁶³ G. B. Sun,⁷⁶
 G. X. Sun,¹ H. Sun,⁶³ H. K. Sun,¹ J. F. Sun,¹⁹ K. Sun,⁶¹ L. Sun,⁷⁶ S. S. Sun,^{1,63} T. Sun,^{51,f} W. Y. Sun,³⁴ Y. Sun,⁹ Y. J. Sun,^{71,58}
 Y. Z. Sun,¹ Z. Q. Sun,^{1,63} Z. T. Sun,⁵⁰ C. J. Tang,⁵⁴ G. Y. Tang,¹ J. Tang,⁵⁹ M. Tang,^{71,58} Y. A. Tang,⁷⁶ L. Y. Tao,⁷²
 Q. T. Tao,^{25,i} M. Tat,⁶⁹ J. X. Teng,^{71,58} V. Thoren,⁷⁵ W. H. Tian,⁵⁹ Y. Tian,^{31,63} Z. F. Tian,⁷⁶ I. Uman,^{62b} Y. Wan,⁵⁵
 S. J. Wang,⁵⁰ B. Wang,¹ B. L. Wang,⁶³ Bo Wang,^{71,58} D. Y. Wang,^{46,h} F. Wang,⁷² H. J. Wang,^{38,k,l} J. J. Wang,⁷⁶ J. P. Wang,⁵⁰
 K. Wang,^{1,58} L. L. Wang,¹ M. Wang,⁵⁰ N. Y. Wang,⁶³ S. Wang,^{12,g} S. Wang,^{38,k,l} T. Wang,^{12,g} T. J. Wang,⁴³ W. Wang,⁵⁹
 W. Wang,⁷² W. P. Wang,^{35,71,o} X. Wang,^{46,h} X. F. Wang,^{38,k,l} X. J. Wang,³⁹ X. L. Wang,^{12,g} X. N. Wang,¹ Y. Wang,⁶¹
 Y. D. Wang,⁴⁵ Y. F. Wang,^{1,58,63} Y. L. Wang,¹⁹ Y. N. Wang,⁴⁵ Y. Q. Wang,¹ Yaqian Wang,¹⁷ Yi Wang,⁶¹ Z. Wang,^{1,58}
 Z. L. Wang,⁷² Z. Y. Wang,^{1,63} Ziyi Wang,⁶³ D. H. Wei,¹⁴ F. Weidner,⁶⁸ S. P. Wen,¹ Y. R. Wen,³⁹ U. Wiedner,³ G. Wilkinson,⁶⁹
 M. Wolke,⁷⁵ L. Wollenberg,³ C. Wu,³⁹ J. F. Wu,^{1,8} L. H. Wu,¹ L. J. Wu,^{1,63} X. Wu,^{12,g} X. H. Wu,³⁴ Y. Wu,^{71,58} Y. H. Wu,⁵⁵
 Y. J. Wu,³¹ Z. Wu,^{1,58} L. Xia,^{71,58} X. M. Xian,³⁹ B. H. Xiang,^{1,63} T. Xiang,^{46,h} D. Xiao,^{38,k,l} G. Y. Xiao,⁴² S. Y. Xiao,¹
 Y. L. Xiao,^{12,g} Z. J. Xiao,⁴¹ C. Xie,⁴² X. H. Xie,^{46,h} Y. Xie,⁵⁰ Y. G. Xie,^{1,58} Y. H. Xie,⁶ Z. P. Xie,^{71,58} T. Y. Xing,^{1,63}
 C. F. Xu,^{1,63} C. J. Xu,⁵⁹ G. F. Xu,¹ H. Y. Xu,^{66,2,p} M. Xu,^{71,58} Q. J. Xu,¹⁶ Q. N. Xu,³⁰ W. Xu,¹ W. L. Xu,⁶⁶ X. P. Xu,⁵⁵

Y. C. Xu,⁷⁷ Z. S. Xu,⁶³ F. Yan,^{12,g} L. Yan,^{12,g} W. B. Yan,^{71,58} W. C. Yan,⁸⁰ X. Q. Yan,¹ H. J. Yang,^{51,f} H. L. Yang,³⁴ H. X. Yang,¹ T. Yang,¹ Y. Yang,^{12,g} Y. F. Yang,^{1,63} Y. F. Yang,⁴³ Y. X. Yang,^{1,63} Z. W. Yang,^{38,k,l} Z. P. Yao,⁵⁰ M. Ye,^{1,58} M. H. Ye,⁸ J. H. Yin,¹ Z. Y. You,⁵⁹ B. X. Yu,^{1,58,63} C. X. Yu,⁴³ G. Yu,^{1,63} J. S. Yu,^{25,i} T. Yu,⁷² X. D. Yu,^{46,h} Y. C. Yu,⁸⁰ C. Z. Yuan,^{1,63} J. Yuan,³⁴ J. Yuan,⁴⁵ L. Yuan,² S. C. Yuan,^{1,63} Y. Yuan,^{1,63} Z. Y. Yuan,⁵⁹ C. X. Yue,³⁹ A. A. Zafar,⁷³ F. R. Zeng,⁵⁰ S. H. Zeng,⁷² X. Zeng,^{12,g} Y. Zeng,^{25,i} Y. J. Zeng,⁵⁹ Y. J. Zeng,^{1,63} X. Y. Zhai,³⁴ Y. C. Zhai,⁵⁰ Y. H. Zhan,⁵⁹ A. Q. Zhang,^{1,63} B. L. Zhang,^{1,63} B. X. Zhang,¹ D. H. Zhang,⁴³ G. Y. Zhang,¹⁹ H. Zhang,⁸⁰ H. Zhang,^{71,58} H. C. Zhang,^{1,58,63} H. H. Zhang,³⁴ H. H. Zhang,⁵⁹ H. Q. Zhang,^{1,58,63} H. R. Zhang,^{71,58} H. Y. Zhang,^{1,58} J. Zhang,⁸⁰ J. Zhang,⁵⁹ J. J. Zhang,⁵² J. L. Zhang,²⁰ J. Q. Zhang,⁴¹ J. S. Zhang,^{12,g} J. W. Zhang,^{1,58,63} J. X. Zhang,^{38,k,l} J. Y. Zhang,¹ J. Z. Zhang,^{1,63} Jianyu Zhang,⁶³ L. M. Zhang,⁶¹ Lei Zhang,⁴² P. Zhang,^{1,63} Q. Y. Zhang,³⁴ R. Y. Zhang,^{38,k,l} S. H. Zhang,^{1,63} Shulei Zhang,^{25,i} X. D. Zhang,⁴⁵ X. M. Zhang,¹ X. Y. Zhang,⁵⁰ Y. Zhang,⁷² Y. Zhang,¹ Y. T. Zhang,⁸⁰ Y. H. Zhang,^{1,58} Y. M. Zhang,³⁹ Yan Zhang,^{71,58} Z. D. Zhang,¹ Z. H. Zhang,¹ Z. L. Zhang,³⁴ Z. Y. Zhang,⁷⁶ Z. Y. Zhang,⁴³ Z. Z. Zhang,⁴⁵ G. Zhao,¹ J. Y. Zhao,^{1,63} J. Z. Zhao,^{1,58} L. Zhao,¹ Lei Zhao,^{71,58} M. G. Zhao,⁴³ N. Zhao,⁷⁸ R. P. Zhao,⁶³ S. J. Zhao,⁸⁰ Y. B. Zhao,^{1,58} Y. X. Zhao,^{31,63} Z. G. Zhao,^{71,58} A. Zhemchugov,^{36,b} B. Zheng,⁷² B. M. Zheng,³⁴ J. P. Zheng,^{1,58} W. J. Zheng,^{1,63} Y. H. Zheng,⁶³ B. Zhong,⁴¹ X. Zhong,⁵⁹ H. Zhou,⁵⁰ J. Y. Zhou,³⁴ L. P. Zhou,^{1,63} S. Zhou,⁶ X. Zhou,⁷⁶ X. K. Zhou,⁶ X. R. Zhou,^{71,58} X. Y. Zhou,³⁹ Y. Z. Zhou,^{12,g} J. Zhu,⁴³ K. Zhu,¹ K. J. Zhu,^{1,58,63} K. S. Zhu,^{12,g} L. Zhu,³⁴ L. X. Zhu,⁶³ S. H. Zhu,⁷⁰ T. J. Zhu,^{12,g} W. D. Zhu,⁴¹ Y. C. Zhu,^{71,58} Z. A. Zhu,^{1,63} J. H. Zou,¹ and J. Zu^{71,58}

(BESIII Collaboration)

¹*Institute of High Energy Physics, Beijing 100049, People's Republic of China*²*Beihang University, Beijing 100191, People's Republic of China*³*Bochum Ruhr-University, D-44780 Bochum, Germany*⁴*Budker Institute of Nuclear Physics SB RAS (BINP), Novosibirsk 630090, Russia*⁵*Carnegie Mellon University, Pittsburgh, Pennsylvania 15213, USA*⁶*Central China Normal University, Wuhan 430079, People's Republic of China*⁷*Central South University, Changsha 410083, People's Republic of China*⁸*China Center of Advanced Science and Technology, Beijing 100190, People's Republic of China*⁹*China University of Geosciences, Wuhan 430074, People's Republic of China*¹⁰*Chung-Ang University, Seoul, 06974, Republic of Korea*¹¹*COMSATS University Islamabad, Lahore Campus,**Defence Road, Off Raiwind Road, 54000 Lahore, Pakistan*¹²*Fudan University, Shanghai 200433, People's Republic of China*¹³*GSI Helmholtzcentre for Heavy Ion Research GmbH, D-64291 Darmstadt, Germany*¹⁴*Guangxi Normal University, Guilin 541004, People's Republic of China*¹⁵*Guangxi University, Nanning 530004, People's Republic of China*¹⁶*Hangzhou Normal University, Hangzhou 310036, People's Republic of China*¹⁷*Hebei University, Baoding 071002, People's Republic of China*¹⁸*Helmholtz Institute Mainz, Staudinger Weg 18, D-55099 Mainz, Germany*¹⁹*Henan Normal University, Xinxiang 453007, People's Republic of China*²⁰*Henan University, Kaifeng 475004, People's Republic of China*²¹*Henan University of Science and Technology, Luoyang 471003, People's Republic of China*²²*Henan University of Technology, Zhengzhou 450001, People's Republic of China*²³*Huangshan College, Huangshan 245000, People's Republic of China*²⁴*Hunan Normal University, Changsha 410081, People's Republic of China*²⁵*Hunan University, Changsha 410082, People's Republic of China*²⁶*Indian Institute of Technology Madras, Chennai 600036, India*²⁷*Indiana University, Bloomington, Indiana 47405, USA*^{28a}*INFN Laboratori Nazionali di Frascati, I-00044, Frascati, Italy*^{28b}*INFN Sezione di Perugia, I-06100, Perugia, Italy*^{28c}*University of Perugia, I-06100, Perugia, Italy*^{29a}*INFN Sezione di Ferrara, I-44122, Ferrara, Italy*^{29b}*University of Ferrara, I-44122, Ferrara, Italy*³⁰*Inner Mongolia University, Hohhot 010021, People's Republic of China*³¹*Institute of Modern Physics, Lanzhou 730000, People's Republic of China*³²*Institute of Physics and Technology, Peace Avenue 54B, Ulaanbaatar 13330, Mongolia*³³*Instituto de Alta Investigación, Universidad de Tarapacá, Casilla 7D, Arica 1000000, Chile*

- ³⁴*Jilin University, Changchun 130012, People's Republic of China*
- ³⁵*Johannes Gutenberg University of Mainz, Johann-Joachim-Becher-Weg 45, D-55099 Mainz, Germany*
- ³⁶*Joint Institute for Nuclear Research, 141980 Dubna, Moscow region, Russia*
- ³⁷*Justus-Liebig-Universitaet Giessen, II. Physikalisches Institut, Heinrich-Buff-Ring 16, D-35392 Giessen, Germany*
- ³⁸*Lanzhou University, Lanzhou 730000, People's Republic of China*
- ³⁹*Liaoning Normal University, Dalian 116029, People's Republic of China*
- ⁴⁰*Liaoning University, Shenyang 110036, People's Republic of China*
- ⁴¹*Nanjing Normal University, Nanjing 210023, People's Republic of China*
- ⁴²*Nanjing University, Nanjing 210093, People's Republic of China*
- ⁴³*Nankai University, Tianjin 300071, People's Republic of China*
- ⁴⁴*National Centre for Nuclear Research, Warsaw 02-093, Poland*
- ⁴⁵*North China Electric Power University, Beijing 102206, People's Republic of China*
- ⁴⁶*Peking University, Beijing 100871, People's Republic of China*
- ⁴⁷*Qufu Normal University, Qufu 273165, People's Republic of China*
- ⁴⁸*Renmin University of China, Beijing 100872, People's Republic of China*
- ⁴⁹*Shandong Normal University, Jinan 250014, People's Republic of China*
- ⁵⁰*Shandong University, Jinan 250100, People's Republic of China*
- ⁵¹*Shanghai Jiao Tong University, Shanghai 200240, People's Republic of China*
- ⁵²*Shanxi Normal University, Linfen 041004, People's Republic of China*
- ⁵³*Shanxi University, Taiyuan 030006, People's Republic of China*
- ⁵⁴*Sichuan University, Chengdu 610064, People's Republic of China*
- ⁵⁵*Soochow University, Suzhou 215006, People's Republic of China*
- ⁵⁶*South China Normal University, Guangzhou 510006, People's Republic of China*
- ⁵⁷*Southeast University, Nanjing 211100, People's Republic of China*
- ⁵⁸*State Key Laboratory of Particle Detection and Electronics, Beijing 100049, Hefei 230026, People's Republic of China*
- ⁵⁹*Sun Yat-Sen University, Guangzhou 510275, People's Republic of China*
- ⁶⁰*Suranaree University of Technology, University Avenue 111, Nakhon Ratchasima 30000, Thailand*
- ⁶¹*Tsinghua University, Beijing 100084, People's Republic of China*
- ^{62a}*Turkish Accelerator Center Particle Factory Group, Istinye University, 34010, Istanbul, Turkey*
- ^{62b}*Near East University, Nicosia, North Cyprus, 99138, Mersin 10, Turkey*
- ⁶³*University of Chinese Academy of Sciences, Beijing 100049, People's Republic of China*
- ⁶⁴*University of Groningen, NL-9747 AA Groningen, The Netherlands*
- ⁶⁵*University of Hawaii, Honolulu, Hawaii 96822, USA*
- ⁶⁶*University of Jinan, Jinan 250022, People's Republic of China*
- ⁶⁷*University of Manchester, Oxford Road, Manchester, M13 9PL, United Kingdom*
- ⁶⁸*University of Muenster, Wilhelm-Klemm-Strasse 9, 48149 Muenster, Germany*
- ⁶⁹*University of Oxford, Keble Road, Oxford OX13RH, United Kingdom*
- ⁷⁰*University of Science and Technology Liaoning, Anshan 114051, People's Republic of China*
- ⁷¹*University of Science and Technology of China, Hefei 230026, People's Republic of China*
- ⁷²*University of South China, Hengyang 421001, People's Republic of China*
- ⁷³*University of the Punjab, Lahore-54590, Pakistan*
- ^{74a}*University of Turin and INFN, University of Turin, I-10125, Turin, Italy*
- ^{74b}*University of Eastern Piedmont, I-15121, Alessandria, Italy*
- ^{74c}*INFN, I-10125, Turin, Italy*
- ⁷⁵*Uppsala University, Box 516, SE-75120 Uppsala, Sweden*
- ⁷⁶*Wuhan University, Wuhan 430072, People's Republic of China*
- ⁷⁷*Yantai University, Yantai 264005, People's Republic of China*
- ⁷⁸*Yunnan University, Kunming 650500, People's Republic of China*
- ⁷⁹*Zhejiang University, Hangzhou 310027, People's Republic of China*
- ⁸⁰*Zhengzhou University, Zhengzhou 450001, People's Republic of China*

^aDeceased.^bAlso at the Moscow Institute of Physics and Technology, Moscow 141700, Russia.^cAlso at the Novosibirsk State University, Novosibirsk, 630090, Russia.^dAlso at the NRC "Kurchatov Institute," PNPI, 188300, Gatchina, Russia.^eAlso at Goethe University Frankfurt, 60323 Frankfurt am Main, Germany.^fAlso at Key Laboratory for Particle Physics, Astrophysics and Cosmology, Ministry of Education; Shanghai Key Laboratory for Particle Physics and Cosmology; Institute of Nuclear and Particle Physics, Shanghai 200240, People's Republic of China.

^gAlso at Key Laboratory of Nuclear Physics and Ion-beam Application (MOE) and Institute of Modern Physics, Fudan University, Shanghai 200443, People's Republic of China.

^hAlso at State Key Laboratory of Nuclear Physics and Technology, Peking University, Beijing 100871, People's Republic of China.

ⁱAlso at School of Physics and Electronics, Hunan University, Changsha 410082, China.

^jAlso at Guangdong Provincial Key Laboratory of Nuclear Science, Institute of Quantum Matter, South China Normal University, Guangzhou 510006, China.

^kAlso at MOE Frontiers Science Center for Rare Isotopes, Lanzhou University, Lanzhou 730000, People's Republic of China.

^lAlso at Lanzhou Center for Theoretical Physics, Lanzhou University, Lanzhou 730000, People's Republic of China.

^mAlso at the Department of Mathematical Sciences, IBA, Karachi 75270, Pakistan.

ⁿAlso at Ecole Polytechnique Federale de Lausanne (EPFL), CH-1015 Lausanne, Switzerland.

^oAlso at Helmholtz Institute Mainz, Staudinger Weg 18, D-55099 Mainz, Germany.

^pAlso at School of Physics, Beihang University, Beijing 100191, China.